

**EFFECT OF ALKALINE EARTH METAL
CATIONS INCORPORATION ON THE SELF-
ASSEMBLY OF MESOPOROUS SILICA:
PHYSICOCHEMICAL STUDY AND CATALYSIS
OF STYRENE**

TAN KOK HOU

UNIVERSITI SAINS MALAYSIA

2021

**EFFECT OF ALKALINE EARTH METAL
CATIONS INCORPORATION ON THE SELF-
ASSEMBLY OF MESOPOROUS SILICA:
PHYSICOCHEMICAL STUDY AND CATALYSIS
OF STYRENE**

by

TAN KOK HOU

**Thesis submitted in fulfillment of the requirements
for the degree of
Doctor of Philosophy**

January 2021

ACKNOWLEDGEMENT

I would like to thank my supervisor, Dr Mohammad Anwar Mohammed Iqbal, for his guidance and support towards the completion of my study. I would also like to extend my gratitude to my co-supervisors, Associate Professor Dr Noor Hana Hanif Abu Bakar and Professor Farook Adam, for their constructive advice.

I would also like to give my appreciation to my lab mates, Dr Wong Jia Tian and Ms Nur Ruzaina Abdul Rahman for their help on the use of gas chromatography and XPS analysis. I would like to extend my appreciation to the staff and lab officers of the School of Chemical Sciences, USM for their supports during my study.

I would like to acknowledge the financial supports from the Ministry of Education Malaysia (Higher Education) and Universiti Sains Malaysia (USM) through USM Short Term Grant (304/PKIMIA/6313215), Universiti Sains Malaysia Research University Grant (RUI) (1001/PKIMIA/8011083), Fundamental Research Grant Scheme (FRGS) (203/PKIMIA/6711790) and Trans-disciplinary Research Grant Scheme (TRGS) (203/PKIMIA/679001). Appreciation is also given to RSC Materials Chemistry Division for the financial support through Travel Grant for PhD Students and Early Career Scientists to participate 5th RSC Early Career Symposium. Travel grant from the RSC Malaysia Local Section to present my work at 19th Malaysian International Chemical Congress (MICC), at Langkawi, Kedah was also appreciated.

Lastly, I would also like to dedicate my deep gratitude to my dearest wife, Chee Ying, for her love, encouragement and support to me throughout the time of this research.

TABLE OF CONTENTS

ACKNOWLEDGEMENT	ii
TABLE OF CONTENTS	iii
LIST OF TABLES	viii
LIST OF FIGURES	x
LIST OF SCHEMES	xv
LIST OF ABBREVIATIONS	xvi
LIST OF SYMBOLS	xviii
LIST OF APPENDICES	xix
ABSTRAK	xxi
ABSTACT	xxii
CHAPTER 1 INTRODUCTION	1
1.1 Catalyst.....	1
1.2 Alkene epoxidation	2
1.3 Epoxidation of styrene	3
1.4 Applications of styrene oxide.....	4
1.5 Catalyst for styrene epoxidation	5
1.5.1 Biocatalyst.....	5
1.5.2 Homogeneous catalyst	5
1.5.3 Heterogeneous catalyst.....	6
1.6 Metal-catalysed styrene epoxidation.....	6
1.6.1 Organometallic complexes.....	8
1.6.2 Metal oxides	9
1.6.3 Metal-Organic Framework (MOF) materials.....	10
1.6.4 Supported metals	11
1.6.4(a) Zeolites as a catalyst support	12
1.6.4(b) Mesoporous silica as catalyst support	13
1.6.4(c) Other supports.....	16

1.7	Reaction mechanism	19
1.8	Mesoporous silica support	22
1.8.1	Metal Incorporated Silica.....	24
1.9	Scope of research	27
1.10	Problem statement.....	27
1.11	Objectives.....	29
CHAPTER 2 EXPERIMENTAL		30
2.1	Materials.....	30
2.2	Preparation and modification of silica support from rice husk ash (RHA).....	30
2.2.1	Preparation of RHA	30
2.2.2	Synthesis of mesoporous silica (MST)	31
2.2.3	Direct one-pot synthesis of mesoporous alkaline earth metal (Mg, Ca, Ba) silicates.....	31
2.3	Catalysts characterization.....	32
2.3.1	Scanning electron microscope (SEM) analysis.....	32
2.3.2	Transmission electron microscope (TEM) analysis.....	33
2.3.3	Powder X-ray diffraction (PXRD) analysis.....	33
2.3.4	Nitrogen adsorption-desorption analysis	33
2.3.5	Elemental analysis	34
2.3.6	Chemical environment analysis	35
2.4	Catalytic Testing	35
2.4.1	Kinetics study.....	37
2.4.2	Reusability Study	39
CHAPTER 3 DIRECT ONE-POT SYNTHESIS OF MESOPOROUS MAGNESIUM SILICATE FOR CATALYZING LIQUID PHASE STYRENE EPOXIDATION WITH H₂O₂.....		40
3.1	Introduction.....	40
3.2	Catalysts characterization.....	40
3.2.1	Elemental analysis using inductively coupled plasma optical emission spectroscopy (ICP-OES) and X-ray photoelectron spectroscopy (XPS) analyses	40

3.2.2	Powder X-ray diffraction (XRD) analysis	41
3.2.3	Surface environmental and metal coordination using X-ray photoelectron spectroscopy (XPS) analysis	43
3.2.4	Nitrogen adsorption-desorption analysis	48
3.2.5	Electron microscopy	50
3.2.6	Fourier transform infrared (FT-IR) spectroscopy	53
3.3	Catalytic testing.....	54
3.3.1	Epoxidation of styrene	54
3.3.2	Effect of reaction time.....	55
3.3.3	Effect of Mg/CTAB molar ratio.....	56
3.3.4	Effect of reactant ratio.....	58
3.3.5	Effect of catalyst loading	59
3.3.6	Effect of temperature.....	60
3.3.7	Kinetics study.....	63
3.3.8	Reusability test.....	66
3.3.9	Proposed reaction mechanism.....	66
3.4	Summary	69
CHAPTER 4 INFLUENCE OF CALCIUM CONTENT ON THE PHYSICO-CHEMICAL PROPERTIES OF MESOPOROUS SILICA AND ITS CATALYTIC PERFORMANCE IN STYRENE EPOXIDATION		71
4.1	Introduction	71
4.2	Catalyst characterization	71
4.2.1	Elemental analysis using inductively coupled plasma optical emission spectroscopy (ICP-OES) and X-ray photoelectron spectroscopy (XPS) analyses	71
4.2.2	Powder X-ray diffraction (XRD) analysis	72
4.2.3	Surface environmental and metal coordination using X-ray photoelectron spectroscopy (XPS) analysis	74
4.2.4	Nitrogen adsorption-desorption analysis	77
4.2.5	Electron microscopy	79
4.2.6	Fourier transform infrared (FT-IR) spectroscopy	82
4.3	Catalytic testing.....	84

4.3.1	Effect of Ca/CTAB molar ratio.....	85
4.3.2	Effect of styrene to H ₂ O ₂ molar ratio.....	86
4.3.3	Effect of catalyst loading	88
4.3.4	Effect of reaction time.....	89
4.3.5	Effect of reaction temperature.....	90
4.3.6	Kinetic Studies	92
4.3.7	Heterogeneity and recyclability	93
4.3.8	Proposed reaction mechanism.....	95
4.4	Summary	99
CHAPTER 5 SYNTHESIS AND CHARACTERIZATION OF BUBBLE WRAP-LIKE BARIUM SILICATE HOLLOW NANOSPHERES FOR CATALYTIC STYRENE EPOXIDATION		100
5.1	Introduction	100
5.2	Catalyst characterization	100
5.2.1	Elemental analysis using inductively coupled plasma optical emission spectroscopy (ICP-OES) and X-ray photoelectron spectroscopy (XPS) analyses	100
5.2.2	Powder X-ray diffraction (XRD) analysis	101
5.2.3	Surface environmental and metal coordination using X- ray photoelectron spectroscopy (XPS) analysis.....	103
5.2.4	Nitrogen adsorption-desorption analysis	106
5.2.5	Electron microscopy	108
5.2.6	Fourier transform infrared (FT-IR) spectroscopy	110
5.3	Proposed formation mechanism of barium silicate hollow nanospheres.....	112
5.4	Catalytic testing.....	113
5.4.1	Effect of Ba/CTAB molar ratio.....	113
5.4.2	Effect of styrene to H ₂ O ₂ molar ratio.....	116
5.4.3	Effect of catalyst loading	118
5.4.4	Effect of reaction temperature.....	120
5.4.5	Kinetic Studies	121
5.4.6	Heterogeneity and recyclability	124
5.4.7	Proposed reaction mechanism.....	126

5.4.8	Comparison between 1.00MgMST, 1.00CaMST and 1.00BaMST	128
5.5	Summary	132
CHAPTER 6 CONCLUSION AND FUTURE WORKS.....		134
6.1	Conclusions	134
6.2	Recommendation for future work	136
REFERENCES.....		138
APPENDICES		
LIST OF PUBLICATIONS		

LIST OF TABLES

	Page
Table 1.1 Types of styrene epoxidation catalyst and the best performed candidate discussed in the text	7
Table 2.1 List of chemicals used in the project.....	30
Table 2.2 Mass of alkaline earth metal nitrate salts added to CTAB solution at specified metal/CTAB ratio	32
Table 2.3 Characteristic wavelengths of alkaline earth in ICP-OES analysis	34
Table 2.4 Reaction kinetic model and their integrated rate laws used in this study	38
Table 3.1 Magnesium content of MgMST catalysts measured using ICP-OES and XPS.....	41
Table 3.2 Lattice parameters of MST and MgMST catalysts	43
Table 3.3 The XPS data of Mg 1s, Si 2p, O 1s and C 1s of the catalysts. Energy calibrated with hydrocarbon C 1s peak position at 284.8 eV ...	47
Table 3.4 The textural properties of MST and MgMST catalysts determined from nitrogen adsorption-desorption analysis.....	49
Table 3.5 Catalytic performance of blank, mesoporous silica (MST), and mesoporous magnesium silicate (1.00MgMST)	62
Table 3.6 The rate constant and adjusted R-square of 1.00MgMST catalysed styrene epoxidation reaction fitted into selected kinetic models at 333 K, 353 K and 373 K	63
Table 3.7 Styrene epoxidation reaction activation energy of several catalytic systems and of 1.00MgMST	65
Table 4.1 Calcium content of CaMST nanoparticles measured by two methods of different depth resolution.....	72

Table 4.2	Ca 2p, Si 2p, O 1s and C 1s XPS spectrum of CaMST. Binding energy calibrated with hydrocarbon C 1s peak position=284.8 eV	76
Table 4.3	BET results of mesoporous calcium silicate	79
Table 4.4	Catalytic performance of blank, MST and 1.00CaMST under optimum condition	92
Table 4.5	Rate constant and adjusted R-square of experimental data fitted in different kinetic model	93
Table 5.1	Comparison between the barium content in BaMST catalysts measured by using ICP-OES and XPS	101
Table 5.2	Crystallite size (d_{XRD}) of witherite phase determined using the Scherrer equation	103
Table 5.3	Binding energy of Ba 3d _{5/2} , Si 2p, O 1s and C 1s of prepared BaMST	104
Table 5.4	The N ₂ sorption surface analysis parameters for 0.25BaMST, 0.50BaMST, 0.75BaMST and 1.00BaMST	108
Table 5.5	Catalytic performance of blank, MST, and 1.00BaMST under optimum condition	124
Table 5.6	Comparison between the physicochemical properties and catalytic activity of 1.00MgMST, 1.00CaMST, and 1.00BaMST.....	129

LIST OF FIGURES

	Page
Figure 1.1 Schematic illustration of the types of catalysts	2
Figure 1.2 Possible products of styrene epoxidation	4
Figure 1.3 Reaction mechanism of hydrogen peroxide activation through (a) one-electron transfer, (b) formation of metal hydroperoxide complex, and (c) formation of metal hydroperoxide	21
Figure 1.4 Schematic presentation of MCM-41 synthesis, an example of liquid crystal templating synthesis of mesoporous silica	23
Figure 2.1 Linear plot of integrated rate law of (a) zero order, (b) first order, (c) second order, (d) pseudo-first-order, and (e) pseudo-second-order kinetic model	38
Figure 3.1 The XRD diffractograms of MST and MgMST catalysts at (a) small and (b) wide angle.....	42
Figure 3.2 XPS spectra of 1.00MgMST at the binding energy of (a) Mg 1s, (b) Si 2p, (c) O 1s, and (d) C 1s.....	44
Figure 3.3 The possible structure of magnesium in (a) enstatite, (b) forsterite, (c) magnesium silicate-carbonate, and (d) Mg-O ₃ Si based on XPS analysis	47
Figure 3.4 The nitrogen adsorption and desorption isotherms of MST and MgMST catalysts.....	48
Figure 3.5 The TEM micrographs of (a) MST, (b) 0.25MgMST, (c) 0.50MgMST, (d) 0.75MgMST and (e) 1.00MgMST. Scale bar =50 nm.....	51
Figure 3.6 The SEM micrographs of (a) MST, (b) 0.25MgMST, (c) 0.50MgMST, (d) 0.75MgMST and (e) 1.00MgMST. Scale bar=1 μ m	52

Figure 3.7	FT-IR spectra of mesoporous silica (MST) and mesoporous magnesium silicate (MgMST).....	53
Figure 3.8	GC-MS chromatogram of mesoporous magnesium silicate catalysed reaction products. In the chromatogram, the mass spectrum of each peak shows the presence of (a) styrene, (b) benzaldehyde (PhCHO), (c) phenylacetaldehyde (PA), and (d) styrene oxide (StO).....	55
Figure 3.9	Evolution of styrene conversion and product selectivity with respect to time using 1.00MgMST nanoparticles as catalyst. Reaction condition: 50 mg of catalyst, 10 mmol of styrene, 20 mmol of H ₂ O ₂ (styrene:H ₂ O ₂ ratio=1:2), 10 mL of acetonitrile and reaction conducted at 80 °C.....	56
Figure 3.10	Effect of Mg/CTAB ratio on styrene conversion and styrene oxide selectivity of catalyst. Reaction condition: 50 mg of catalyst, 10 mL of acetonitrile, 10 mmol of styrene, styrene/H ₂ O ₂ ratio = 1:2, T = 80 °C, t = 1 h, stirring speed = 250 rpm.....	57
Figure 3.11	Effect of styrene/H ₂ O ₂ ratio on the styrene conversion and selectivity of styrene oxide. Reaction condition: 50 mg of 1.00MgMST, 10 mL of acetonitrile, 10 mmol of styrene, T = 80 °C, t = 1 h, stirring speed = 250 rpm	59
Figure 3.12	Effect of catalyst loading on the styrene conversion and selectivity of styrene oxide. Reaction condition: 10 mmol of styrene, 10 mL of acetonitrile, styrene:H ₂ O ₂ ratio = 1:6, T = 80 °C, t = 1 h, stirring speed = 250 rpm	60
Figure 3.13	Styrene conversion and product selectivity after 1 h of reaction at 60, 80 and 100 °C. Reaction condition: 125 mg of 1.00MgMST, 10 mmol of styrene, 60 mmol of H ₂ O ₂ , and 10 mL of acetonitrile	61
Figure 3.14	Styrene conversion and product selectivity of 1.00MgMST after being regenerated using calcination for up to four cycles. Reaction condition: 125 mg of catalyst, 10 mL of acetonitrile, 10 mmol of	

	styrene, styrene/H ₂ O ₂ ratio = 1:6, T = 80 °C, t = 1 h, stirring speed = 250 rpm	66
Figure 4.1	XRD diffractogram of mesoporous CaMST nanoparticles at (a) small angle (1°-10°) and (b) wide-angle (10°-90°).....	73
Figure 4.2	XPS spectrum of (a) C 1s, (b) Ca 2p, (c) O 1s and (d) Si 2p of 1.00CaMST	74
Figure 4.3	Structures of (a) aragonite and (b) calcite type calcium carbonate active sites on CaMST.....	77
Figure 4.4	Nitrogen adsorption (closed symbols) and desorption (open symbols) isotherms of 0.25 (black), 0.50 (red), 0.75 (green) and 1.00CaMST (blue	78
Figure 4.5	TEM micrographs of (a) 0.25CaMST, (b) 0.50CaMST, (c) 0.75CaMST and (d) 1.00CaMST. Scale bar= 50 nm	81
Figure 4.6	SEM micrographs of (a) 0.25CaMST, (b) 0.50CaMST, (c) 0.75CaMST and (d) 1.00CaMST. Scale Bar= 1 μm	82
Figure 4.7	FT-IR spectra of (a) 0.25CaMST, (b) 0.50CaMST, (c) 0.75CaMST, and (d) 1.00CaMST	83
Figure 4.8	GC-MS chromatogram of CaMST catalysed reaction products. In the chromatogram, the mass spectrum of each peak shows the presence of (a) styrene, (b) benzaldehyde (PhCHO), (c) phenylacetaldehyde (PA), and (d) styrene oxide (StO).....	84
Figure 4.9	Effect of Ca/CTAB ratio on styrene conversion and styrene oxide selectivity of catalyst. Reaction condition: 50 mg of catalyst, 10 mL of acetonitrile, 10 mmol of styrene, styrene/H ₂ O ₂ ratio = 1:2, T = 80 °C, t = 1 h, stirring speed = 250 rpm.....	86
Figure 4.10	Effect of styrene/H ₂ O ₂ ratio on the yield of selectivity of styrene oxide. Reaction condition: 50 mg of 1.00CaMST, 10 mL of acetonitrile, 10 mmol of styrene, T = 80 °C, t = 1 h, stirring speed = 250 rpm	87

Figure 4.11	Effect of catalyst loading on the yield and selectivity of styrene oxide. Reaction condition: 10 mL of acetonitrile, 10 mmol of styrene, styrene/H ₂ O ₂ ratio = 1:6, T = 80 °C, t = 1 h, stirring speed = 250 rpm	89
Figure 4.12	The conversion of styrene and products evolution over reaction time. Reaction condition: 100 mg of 1.00CaMST, 10 mmol of styrene, 10 mL of acetonitrile, styrene/H ₂ O ₂ ratio = 1:6, T = 80 °C, and stirring speed = 250 rpm	90
Figure 4.13	Styrene conversion and product selectivities with respect to the reaction temperature. Reaction condition: 100 mg of 1.00CaMST, 10 mmol of styrene, 10 mL of acetonitrile, styrene:H ₂ O ₂ ratio = 1:6, stirring speed = 250 rpm, reaction time=3 h, reflux	91
Figure 4.14	Reusability of 1.00CaMST in catalysing liquid phase styrene epoxidation for up to four cycles	94
Figure 5.1	The small-angle powder XRD (PXRD) diffractogram from 0.25 to 1.00BaMST	102
Figure 5.2	Wide-angle XRD diffractogram of BaMST catalysts	103
Figure 5.3	X-ray Photoelectron (XPS) spectra of 1.00BaMST for (a) Ba 3d, (b) O 1s, (c) C 1s, and (d) Si 2p.....	104
Figure 5.4	The proposed structure of (a) barium silicate, (b) bidentate barium carbonate, and (c) barium carbonate surface active sites	106
Figure 5.5	Nitrogen adsorption-desorption isotherms of 0.25 (black box), 0.50 (red circle), 0.75 (blue diamond) and 1.00BaMST (green star)	107
Figure 5.6	The TEM micrographs of (a) 0.25 BaMST, (b) 0.50 BaMST, (c) 0.75 BaMST, and (d) 1.00 BaMST. Scale bar=100 nm.....	109
Figure 5.7	The SEM images of (a) 0.25 BaMST, (b) 0.50 BaMST, (c) 0.75 BaMST and (d) 1.00BaMST. Scale bar=1 μm.....	110
Figure 5.8	The FT-IR spectra of BaMST catalysts.....	111
Figure 5.9	Relationship between the catalyst's architecture with Ba/CTAB ratio of (a) 0.25, (b) 0.50 and (c) above 0.75.....	113

Figure 5.10	Influence of Ba/CTAB ratio on the catalyst performance. Reaction condition: 50 mg of catalyst, 10 mmol of styrene, 20 mmol of H ₂ O ₂ , 10 mL of acetonitrile, 80 °C, 1 h, 250 rpm, reflux.....	114
Figure 5.11	GC-MS chromatogram of BaMST catalysed reaction products. In the chromatogram, the mass spectrum of each peak shows the presence of (a) styrene, (b) benzaldehyde (PhCHO), (c) phenylacetaldehyde (PA), and (d) styrene oxide (StO)	116
Figure 5.12	Influence of styrene/H ₂ O ₂ ratio on the catalytic performance of mesoporous barium silicate nanospheres. Reaction condition: 50 mg of 1.00BaMST, 10 mmol of styrene, 10 mL of acetonitrile, 80 °C, 1 h, 250 rpm, reflux	117
Figure 5.13	Influence of catalyst loading on the catalytic performance of mesoporous barium silicate nanospheres. Reaction condition: 1.00BaMST catalyst, 10 mmol of styrene, 60 mmol of H ₂ O ₂ , 10 mL of acetonitrile, 80 °C, 1 h, 250 rpm, reflux	119
Figure 5.14	Influence of reaction temperature on the catalytic performance of mesoporous barium silicate nanospheres. Reaction condition: 125 mg of 1.00BaMST catalyst, 10 mmol of styrene, 60 mmol of H ₂ O ₂ , 10 mL of acetonitrile, 1 h, 250 rpm, reflux	121
Figure 5.15	Influence of reaction time on the catalytic performance of mesoporous barium silicate nanospheres. Reaction condition: 125 mg of 1.00BaMST catalyst, 10 mmol of styrene, 60 mmol of H ₂ O ₂ , 10 mL of acetonitrile, 60 °C, 250 rpm, reflux	122
Figure 5.16	Arrhenius plot of 1.00BaMST catalysed liquid phase styrene epoxidation	123
Figure 5.17	Reusability of catalyst for the first four cycles of epoxidation reaction	125
Figure 5.18	IR spectra of fresh 1.00BaMST catalyst (black) and regenerated catalyst (green)	125

LIST OF SCHEMES

	Page
Scheme 3.1 Proposed reaction mechanism of styrene epoxidation on enstatite magnesium surface group.....	67
Scheme 3.2 Proposed reaction mechanism of styrene epoxidation on magnesium metasilicate surface active sites	68
Scheme 3.3 Proposed reaction mechanism of styrene epoxidation on magnesium carbonate surface active sites	69
Scheme 4.1 Catalytic epoxidation of styrene on calcium silicate surface active sites	96
Scheme 4.2 Catalytic epoxidation of styrene on carbonate-bridged calcium silicate surface active sites.....	97
Scheme 4.3 Catalytic epoxidation of styrene on calcium carbonate surface active sites	98
Scheme 5.1 The proposed reaction mechanism for the epoxidation of styrene catalysed by barium silicate species. The self-decomposition of H ₂ O ₂ molecules were suppressed when H ₂ O ₂ interact with the Ba active sites <i>via</i> the ion-dipole attraction	127
Scheme 5.2 The proposed reaction mechanism for the epoxidation of styrene catalysed by barium carbonate species. The H ₂ O ₂ interact with the Ba active sites through dipole-dipole interaction with carbonate anion	128

LIST OF ABBREVIATIONS

AR	Analytical reagent
BaTNT	Barium titanate nanotubes
BET	Brunauer-Emmett-Teller
BJH	Barrett-Joyner-Halenda
PhCHO	Benzaldehyde
CGAR	Centre for Global Archeological Research
CNTs	Carbon nanotubes
CPS	Counts per second
CTAB	Cetyltrimethylammonium bromide
CVD	Chemical vapour deposition
DFT	Density Functional Theory
FeTAPP	Fe(III) tetra(<i>o</i> -aminophenyl)porphyrin
FT-IR	Fourier-Transform infrared
FWHM	Full width at half maximum
GC-FID	Gas chromatography-Flame ionization detector
GC-MS	Gas chromatography-mass spectroscopy
HV	High vacuum
ICP-OES	Inductively coupled plasma-Optical emission spectroscopy
IR	Infrared
IUPAC	International Union of Pure and Applied Chemistry
KIT-6	Korea Advanced Institute of Science and Technology-6
LDH	Layered double hydroxides
MCM-41	Mobil Composition of Matter No. 41
MOF	Metal-organic framework
MST	Mesoporous silica synthesized with the condition identified in this study

MWCNT	Multi-walled carbon nanotubes
NPYR	N-nitrosopyrrolidine
PA	2-Phenylacetaldehyde
POM	Peroxophosphotungstate
PXRD	Powder X-ray diffraction
RH	Rice husk
RHA	Rice husk ash
rpm	Revolutions per minute
SBA-15	Santa Barbara Amorphous-15
SDA	Structure-directing agent
SEM	Scanning electron microscopy
StO	Styrene oxide
TBHP	Tert-butyl hydroperoxide
TEM	Transmission electron microscopy
TGA	Thermogravimetric analysis
TOF	Turnover frequency
TPSR	Temperature-programmed surface reaction
UHV	Ultra-high vacuum
XPS	X-ray photoelectron spectroscopy
XRD	X-ray diffraction

LIST OF SYMBOLS

a_0	Unit cell parameter
N_2	Nitrogen gas
d_{100}	Pore-to-pore distance recorded in nm
d_{BJH}	BJH pore size based on the adsorption isotherm
E_a	Activation energy
H_2O_2	Hydrogen peroxide
R^2	Adjusted R-square
S_{BET}	Specific BET surface area
V_{total}	Total pore volume
θ	Diffraction angle
λ	Wavelength

LIST OF APPENDICES

- APPENDIX A GC-MS mass spectrum of each components in the styrene epoxidation product mixture. (a) Styrene mass spectrum of sample aliquot (red) and NIST reference (black). (b) Benzaldehyde (PhCHO) mass spectrum of sample aliquot (red) and NIST reference (black). (c) Phenylacetaldehyde (PA) mass spectrum of sample aliquot (red) and NIST reference (black). (d) Styrene oxide (StO) mass spectrum of sample aliquot (red) and NIST reference (black)
- APPENDIX B Mg 1s XPS spectrum of (a) 0.25, (b) 0.50, and (c) 0.75MgMST.
- APPENDIX C Si 2p XPS spectrum of (a) 0.25, (b) 0.50, and (c) 0.75MgMST.
- APPENDIX D O 1s XPS spectrum of (a) 0.25, (b) 0.50, and (c) 0.75MgMST.
- APPENDIX E C 1s XPS spectrum of adventitious carbon in (a) 0.25, (b) 0.50, and (c) 0.75MgMST as calibration reference. Signal at 284.8 eV is attributed to C-C group while peaks at ~286 eV and ~288 eV are assigned to C-O and O=C-O, respectively.
- APPENDIX F GC Chromatogram of (a) blank and (b) MST catalysed reaction product testing under the optimum epoxidation condition of 1.00MgMST.
- APPENDIX G Arrhenius plot of $\ln k$ against $1/T$ for the kinetic study of 1.00MgMST catalysed liquid phase styrene epoxidation.
- APPENDIX H XPS spectrum of (a) C 1s, (b) Ca 2p, (c) O 1s and (d) Si 2p of 0.25CaMST.
- APPENDIX I XPS spectrum of (a) C 1s, (b) Ca 2p, (c) O 1s and (d) Si 2p of 0.50CaMST.
- APPENDIX J XPS spectrum of (a) C 1s, (b) Ca 2p, (c) O 1s and (d) Si 2p of 0.75CaMST.

APPENDIX K	GC Chromatogram of (a) blank and (b) MST catalysed reaction product testing under the optimum epoxidation condition of 1.00CaMST.
APPENDIX L	Arrhenius plot for styrene epoxidation with hydrogen peroxide in the presence of 1.00CaMST at various temperature.
APPENDIX M	X-ray Photoelectron (XPS) spectra of 0.25BaMST for (a) Ba 3d, (b) O 1s, (c) C 1s, and (d) Si 2p.
APPENDIX N	X-ray Photoelectron (XPS) spectra of 0.50BaMST for (a) Ba 3d, (b) O 1s, (c) C 1s, and (d) Si 2p.
APPENDIX O	X-ray Photoelectron (XPS) spectra of 0.75BaMST for (a) Ba 3d, (b) O 1s, (c) C 1s, and (d) Si 2p.
APPENDIX P	Particle Size of Nanospheres and Nanorod
APPENDIX Q	Rate constant and R-square of styrene epoxidation reaction catalysed by 1.00BaMST nanoparticles at different temperature.
APPENDIX R	GC Chromatogram of MST catalysed reaction product testing under the optimum epoxidation condition of 1.00BaMST.

**KESAN PENGGABUNGAN KATION LOGAM ALKALI BUMI KE ATAS
PENSWAPASANGAN SILIKA BERLIANG MESO: KAJIAN FIZIKO KIMIA
DAN PEMANGKINAN STIRENA**

ABSTRAK

Tiga siri mangkin logam alkali bumi (magnesium, kalsium dan barium) silikat berliang meso telah dihasilkan menggunakan kaedah sintesis serentak dengan mengubah nisbah molar logam/ agen pengarah permukaan (CTAB) (0.25, 0.50, 0.75 dan 100). Penggabungan logam alkali bumi ke dalam kekisi silika telah mengubah susunan saluran liang dan meningkatkan saiz liang berbanding silika asal. Spesies logam alkali bumi diatas permukaan pemangkin berubah mengikut nisbah molar logam/CTAB. Pengoksidaan stirena dalam fasa cecair telah menghasilkan stirena oksida (StO) sebagai produk utama manakala benzaldehid (PhCHO) dan fenilasetaldehid (PA) ditemui sebagai produk minor. Secara umumnya, aktiviti yang paling tinggi telah didapati apabila nisbah logam/CTAB bersama dengan 1.00. 1.00CaMST yang berliang meso telah menunjukkan prestasi yang terbaik dengan mencapai penukaran stirena (66.9%) dan kepilihan stirena oksida (79.2%) yang paling tinggi pada suhu sederhana (60 °C) dan muatan mangkin (100 mg) yang lebih rendah. Tenaga pengaktifan 1.00CaMST (10.9 kJ mol⁻¹) didapati lebih rendah berbanding dengan 1.00MgMST (27.7 kJ mol⁻¹) dan 1.00BaMST (17.3 kJ mol⁻¹). Tindak balas tersebut didapati mematuhi model kinetik tertib pseudo-pertama. Mekanisme tindak balas yang dimangkin telah dicadangkan berdasarkan jenis tapak aktif logam alkali bumi.

**EFFECT OF ALKALINE EARTH METAL CATIONS INCORPORATION
ON THE SELF-ASSEMBLY OF MESOPOROUS SILICA:
PHYSICOCHEMICAL STUDY AND CATALYSIS OF STYRENE**

ABSTRACT

Three series of alkaline earth metal (magnesium, calcium and barium) mesoporous silicate catalysts were prepared *via* direct one-pot synthesis by varying the metal to surface directing agent (CTAB) molar ratio (0.25, 0.50, 0.75 and 1.00). Characterization results indicate that the physicochemical properties of the resulting catalysts depend on the size of the alkaline earth metal cations and metal/CTAB molar ratios. The incorporation of the alkaline earth metals in the silica framework disrupted the arrangement of pore channels and increased pore size compared to parent silica (MST). The alkaline earth metal species on the catalyst's surface varies according to the metal/CTAB molar ratio. Liquid phase epoxidation of styrene in the presence of prepared alkaline earth metal catalysts have produced styrene oxide (StO) as the major product and benzaldehyde (PhCHO) and phenylacetaldehyde (PA) as the minor products. In general, the highest catalytic activity was observed at a metal/CTAB ratio of 1.00. Mesoporous 1.00CaMST performed the best by achieving the highest styrene conversion (66.9%) and StO selectivity (79.2%) at mild temperature (60 °C) and a lower catalyst loading (100 mg). The activation energy of 1.00CaMST (10.9 kJ mol⁻¹) is also found to be lower than 1.00MgMST (27.7 kJ mol⁻¹) and 1.00BaMST (17.3kJ mol⁻¹). The reactions were found to fit better to the pseudo-first order kinetic model. The mechanism of the catalysed reaction was proposed based on the type of alkaline earth metal surface active sites.

CHAPTER 1

INTRODUCTION

1.1 Catalyst

According to the International Union of Pure and Applied Chemistry (IUPAC), a catalyst is defined as a substance that increases the rate of a reaction without modifying the overall standard Gibbs energy change in the reaction whereas the process is called catalysis [1]. The term catalysis was coined by Jöns Jakob Berzelius (1779-1848) in 1835 [2]. He stated that catalysis is “the property of exerting on other bodies an action which is very different from chemical affinity. By means of this action, they produce decomposition in bodies, and form new compounds into the composition of which they do not enter”. Catalysts function by altering the reaction pathway and lowering the energy barrier (activation energy) that is required for the reaction to occur. The importance of catalysts in the chemical industry was reflected by its global market value of US\$ 18.8 billion in 2018. This value is forecasted to rise to US\$ 23.9 billion by 2024 according to the Industrial Catalyst Market: Global Industry Trends, Share, Size, Growth, Opportunity and Forecast 2019-2024 report [3].

Catalysts can be divided into three groups: homogeneous, heterogeneous and biocatalysts (Figure 1.1). Homogeneous catalysts exist in the same phase as the reactants (gas or liquid). In contrast, heterogeneous catalysts exist in a different phase from that of the reaction mixture (e.g. solid-liquid or solid-gas). Heterogeneous catalysts can either be metal-based or metal-free. Biocatalyst refers to the use of enzymes, which originally

function to catalyse biochemical reactions in living organisms. The enzymes are three-dimensional proteins containing active binding sites for substrate binding and catalysis.

Compared to homogeneous catalysts and biocatalysts, heterogeneous catalysts are considered a better choice to catalyse various industrially important chemical reactions due to their ease of recovery and cost-effectiveness.

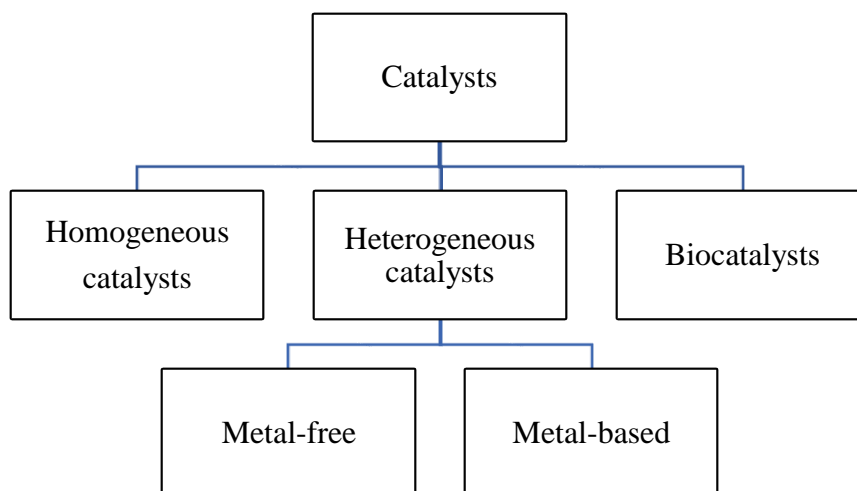


Figure 1.1 Schematic illustration of the types of catalysts.

1.2 Alkene epoxidation

Selective or partial oxidation of hydrocarbons, including saturated alkanes and unsaturated alkenes and alkynes, are of great commercial and synthetic importance. The presence of weak carbon-carbon double bonds in olefins have made them more susceptible towards oxidative functionalization, which is vital to produce valuable products such as epoxides, alcohols, diols, aldehydes, and ketones [4,5]. Nevertheless, catalysts are needed for these chemical reactions to be commercially viable and sustainable. Demands for

active yet affordable catalysts for oxidation reactions has attracted the interest of the research communities since the 1930s.

Alkene epoxidation is the process used to produce reactive epoxide intermediates for pharmaceutical and chemical industries. Due to the instability of the epoxide, mild and clean conditions are particularly important for selective epoxidation processes. Optimum catalyst and oxidant combination are therefore needed to alternate the reaction pathway to a lower activation energy route, which enhances the selectivity and yield of the epoxide.

1.3 Epoxidation of styrene

Styrene oxide (StO) is an epoxide that is of industrial importance. Similar to ethylene oxide and propylene oxide, styrene oxide used to be prepared *via* the chlorohydrin epoxidation route [6,7]. This process needs to be replaced by a more efficient and greener alternative to comply with regulations and increasing demand. So far, various catalytic systems with different combinations of catalysts have been investigated (Section 1.6).

Selectivity is the key to the production of styrene oxide. Styrene oxide, which contains strained epoxy ring and higher bond energy than styrene, is unstable and can be further oxidized to benzaldehyde and benzoic acid through a radical mechanism in the presence of excess oxidant and at higher reaction temperature (Figure 1.2) [8]. In the presence of acid sites, epoxides are prompt to be isomerized to phenylacetaldehyde [9]. The existence of acid sites can also lead to the formation of styrene glycol [10]. Therefore, the design of a catalyst that is selective to the formation of styrene oxide under mild conditions is vital in order to avoid the complication of the product mixture. This can be

achieved by enhancing the rate of StO formation and synthesis of the catalyst with unique surface-active sites that have limited interaction with oxidant or StO.

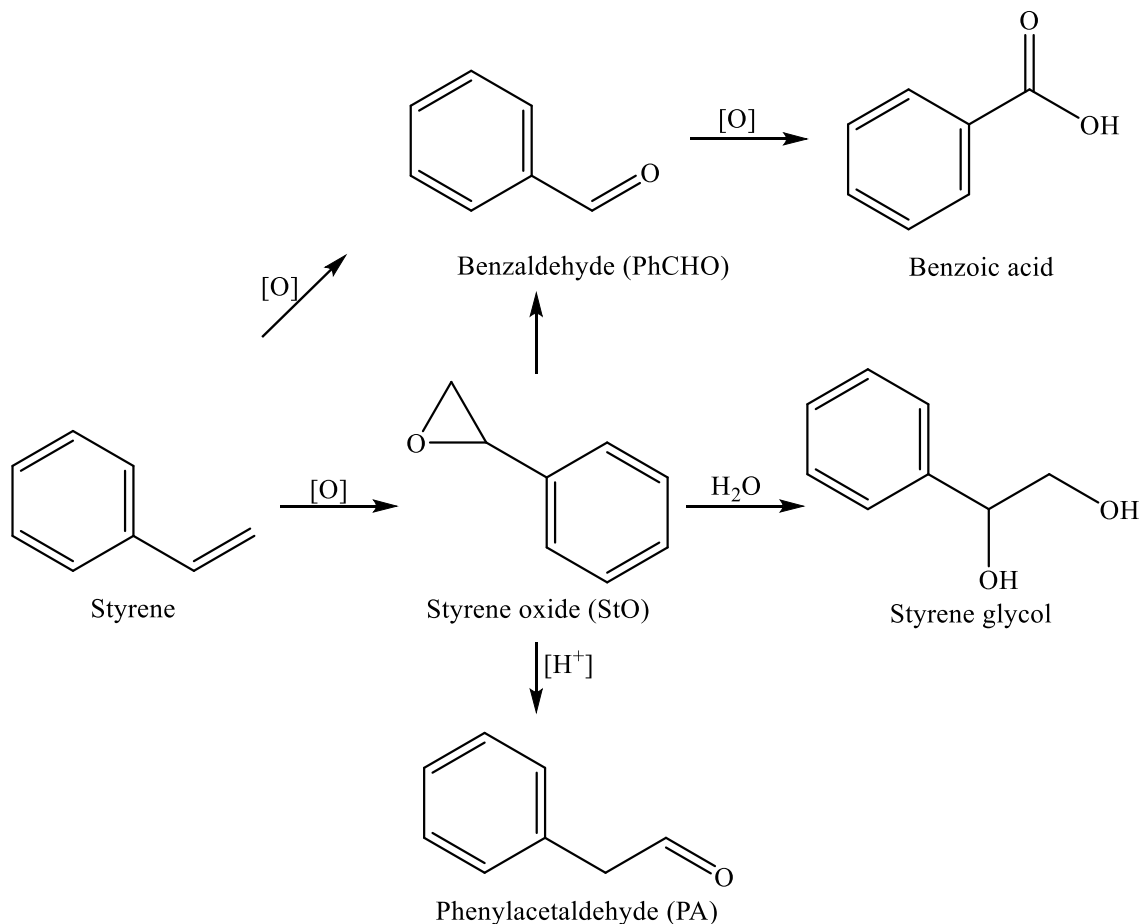


Figure 1.2 Possible products of styrene epoxidation [8–10].

1.4 Applications of styrene oxide

Styrene oxide has been widely used as a precursor or an intermediate in the production of cosmetics, surface coatings, and in the treatment of fibres and textiles. A study by Imai and co-workers [11] reported the use of styrene oxide-based macromonomers in the synthesis of discrete polyethylene oxide-polystyrene oxide microsphere through dispersion copolymerization. Another study by Wu et al. [12] has demonstrated that the cycloaddition of CO₂ to styrene oxide to form alternating

polycarbonate with Co(III) metal complex. Apart from polymerization, the five-membered cyclic styrene carbonate produced *via* CO₂ addition to styrene oxide can also be used as a solvent and fuel additives [13]. In the pharmaceutical industry, styrene oxide is an ingredient for the synthesis of antidepressant and anti-HIV agent [14,15].

1.5 Catalyst for styrene epoxidation

1.5.1 Biocatalyst

In nature, enzymes are used to epoxidize styrene with high yield, excellent chemo-, regio- and enantioselectivities at mild conditions [16]. Styrene monooxygenases bearing either one or two components, which were expressed in microbes such as *Escherichia coli* (*E. coli*), *Pseudomonas* sp. and *Rhodococcus opacus*, have been investigated for biotransformation of styrene to styrene oxide. The relative activity and selectivity of the epoxidation reaction can reach >99% [17,18]. Besides that, cell-free styrene epoxidation has also been studied using monooxygenase and cytochrome P450 enzyme [19,20]. Nevertheless, the high cost of enzyme and reducing equivalents for reductive activation of molecular oxygen are two major limitations for their application in large scale industrial production.

1.5.2 Homogeneous catalyst

Typically, homogeneous catalysis can achieve a good yield at mild conditions. Metal complexes have been frequently employed as homogeneous catalysts. A comprehensive review of the use of transition metal complexes to catalyse epoxidation reactions has been published as early as 1989 [21]. Recent work reported by Díaz-Requejo

and colleagues showed that styrene epoxidation by dihydridobispyrazolylborate copper(I) complex and ozone could yield 70% of styrene oxide with >85% of selectivity [22]. However, the complexity of catalyst synthesis, separation of the catalyst from the reaction mixture and catalyst reusability are the challenges need to be overcome when applying homogeneous catalysis in industry.

1.5.3 Heterogeneous catalyst

Heterogeneous catalysts possess several advantages compared to homogeneous catalysts and biocatalysts. Since heterogeneous catalysts are not in the same phase as the reactants and products, the catalysts can be separated easily and reused several times, and thus making the chemical production process more cost-effective. However, this type of catalysts often suffers from poor catalytic activity and selectivity than their homogeneous counterparts. Much effort has been dedicated in developing new heterogeneous catalysts or improving the existing heterogeneous catalysts for better catalytic performance. These catalysts can be grouped into metal complexes, metal oxide, supported metal and nanoporous catalysts.

1.6 Metal-catalysed styrene epoxidation

Numerous works have been done on identifying metal-based catalysts that are cost-effective, environmentally-friendly as well as feasible for industrial application. The following subsections discuss various examples reported in the literature that contributed to the development of styrene epoxidation catalysts. A summary of the catalyst with the best catalytic performance of each type was displayed in Table 1.1.

Table 1.1 Types of styrene epoxidation catalyst and the best performed candidate discussed in the text.

Catalyst	Oxidant	Loading (mg)	T (°C)	t (h)	Styrene/Oxidant ratio	Styrene Conversion (%)	Epoxide Selectivity (%)	Epoxide Yield (%)	Ref
Insoluble Organometallic Complexes									
Nickel lysine salen complexes with TBHP	TBHP	50	90	10	1:1	91.5	92.0	84.2	[23]
Metal Oxides									
CaO	H ₂ O ₂	60	60	10	1:7	99.2	97.5	96.7	[25]
Supported Metals									
Ag/maghemite	TBHP	20	80	15	1:3	89.6	89.7	80.4	[26]
Sr on Co(II)-exchanged zeolite	O ₂	200	100	4	-	100.0	85.0	85.0	[27]
C8-POM/SBA-15	H ₂ O ₂	500	65	2	1:3	100.0	100.0	100.0	[28]
Au/BaTNT	TBHP	50	80	15	1:1	60.5	80.1	48.5	[29]
Au ₂₅ /Hydroxyapatite	TBHP	50	80	12	1:5.8	100.0	92.0	92.0	[30]
Ag/MgAl-LDH	TBHP	100	82	8	-	80.8	91.1	73.6	[31]
MgO/Carbon	TBHP	100	100	18	1:2	84.0	82.0	68.9	[32]
Metal-Organic Framework (MOF)									
Polytungstate MOF	H ₂ O ₂	39	50	6	1:1.25	73.0	83.0	60.6	[33]

1.6.1 Organometallic complexes

Many works have been conducted to prepare insoluble organometallic complexes for the liquid phase epoxidation processes. A series of period four transition metal lysine salen complexes have been studied for their styrene epoxidation performance with tert-butyl hydroperoxide (TBHP) [23]. The nickel complex achieved the highest conversion and selectivity of 91.51% and 91.99%, respectively for styrene oxide while cobalt counterpart was more selective towards benzaldehyde with a conversion and selectivity of 89.11% and 95.23%, respectively. A unique tungsten-based reaction-controlled phase transfer epoxidation catalyst $[(C_{18}H_{37}(30\%)+C_{16}H_{33}(70\%))N(CH_3)_3]_3-[PW_4O_{16}]$ developed by Yang et al. [24] epoxidized styrene with up to 85% of conversion and >95% of styrene oxide selectivity using H_2O_2 . However, the catalyst was soluble in the presence of H_2O_2 . Despite that, the spent catalyst can be precipitated and recovered with 94.1% recovery efficiency when the oxidant was completely consumed.

1.6.2 Metal oxides

On the other hand, metal oxides have also been frequently used for the epoxidation of styrene. Study on the use of molecular oxygen with Fe_3O_4 shows that styrene conversion and styrene oxide selectivity achieved 38.0% and 56.5%, respectively [34]. Another investigation carried out by Choudhary and co-workers [35] have also tested TiO_2 , Cr_2O_3 , MnO_2 , Fe_2O_3 , CoO , NiO , ZnO , MoO , and U_3O_8 using anhydrous and aqueous TBHP. In their study, NiO showed the best performance (51.7% of conversion, 86.2% of selectivity, 44.6% of yield and $14.9 \text{ g}^{-1} \text{ h}^{-1}$ for TOF). When combined with Co_3O_4 , it was found that NiO can transform 68.0% of styrene to styrene oxide at mild condition (air, $100 \text{ }^\circ\text{C}$, 5 h) [36]. The selectivity of styrene oxide was 86.9%. Higher conversion (>80%) was obtained using bimetallic $\text{Co}_3\text{O}_4\text{-SnO}_x$ and $\text{Co}_3\text{O}_4\text{-ZnO}_x$ with the expenses of selectivity under the same condition. It is worth to note that applying transition metal oxides in combining with H_2O_2 in epoxidation reaction is challenging since they have high activity for the H_2O_2 decomposition and therefore, will give a higher selectivity towards benzaldehyde [37].

Besides transition metals, alkaline earth metal oxides can function as epoxidation catalysts as well. In 2006, Choudhary [38] published a report on the use of different alkaline and rare earth oxides for styrene epoxidation by TBHP. Barium oxide outperformed the others by achieving 40.7% of conversion and 78.7% of styrene oxide selectivity. The reusability test revealed that although the change in styrene oxide selectivity is negligible after five cycles of reuses, the catalytic activity of barium oxide has declined as indicated by a 19% drop in styrene conversion. The authors attributed the superior performance as the result of the relatively easier formation of barium peroxide

when reacting barium oxide with TBHP. Although the activities of magnesium oxide and calcium oxide are low in this study, later investigations conducted using H₂O₂ indicated that both of these oxides are highly active and selective even at mild conditions [25,39]. The amount of very strong basic site and high basic strength were concluded as the two key factors for their exceptional performance. These evidences suggested that alkaline earth metal cations are active catalysts in the epoxidation of styrene.

For Group III metal oxides, their styrene epoxidation activity and epoxide selectivity are low except thallium. The study conducted by Patil and co-workers [40] demonstrated that only Tl₂O₃ exhibits significant conversion and selectivity, both higher than 50%. Styrene conversion by the first three Group III metal oxides, namely Al₂O₃, Ga₂O₃ and In₂O₃, are all below 10% while their epoxide selectivity is between 3-15%. The authors attributed the high catalytic activity and selectivity of Tl₂O₃ as the result of its high basicity and reducibility ($E(\text{Tl}^{3+}/\text{Tl}^{1+}) = +1.25 \text{ V}$), which results in redox-driven styrene epoxidation mechanism. Meanwhile, the results also indicated that metal oxides of lower period members perform better in further oxidising the epoxide to its secondary oxidation products rather than producing the epoxide itself. Hence, it is clearly shown that basicity and reducibility are important factors that decide the styrene epoxidation performance of metal oxide catalyst.

1.6.3 Metal-Organic Framework (MOF) materials

Metal-organic framework (MOF) is an inorganic-organic hybrid material consisting of self-assembly organic ligands and metal ions or clusters. They are promising catalysts owing to their uniform but tuneable cavities, high surface areas, and component

diversification. Several studies have been reported on the catalytic performance of MOF in styrene epoxidation using hydrogen peroxide as oxidant.

The activity of the polytungstate-MOF in catalysing styrene epoxidation was measured by Haddadi and colleagues [33] in the presence of hydrogen peroxide and acetonitrile. They managed to obtain 73% of conversion and 83% of styrene oxide selectivity after 6 h of reaction using this catalyst. On the other hand, high styrene conversion (~99%) and epoxide selectivity (~70%) was obtained by Hui and his co-workers [41] in their study using nitrogen derivatized multicomponent Zn_1Co_1 -ZIF and TBHP in styrene epoxidation. Furthermore, a patent on the use of MOF in the epoxidation of alkenes was filed by BASF and the Regents of the University of Michigan in 2003 [42].

1.6.4 Supported metals

Apart from directly acting as a catalyst, metal oxides can be employed as a support for precious metals in catalysts design. Patil et al. [43] have introduced gold metal onto transition metal oxides *via* the homogeneous deposition-precipitation method. Their results showed that Au/TiO₂ achieved the highest conversion and styrene oxide selectivity among twelve supported metal oxides studied. The catalyst can be reused with the conversion and selectivity maintained closely at 55.9% and 56.3%, respectively for at least six times. Au supported on MgO was shown to perform better than the transition metal oxides and other alkaline earth metal oxides by achieving 67.0% of conversion and 66.1% of selectivity [44]. A latter study by Dumbre et al. [45] on the use of nanogold supported on CaO has managed to reach a higher conversion of 67.6% and 18% higher selectivity than that of Au/MgO. The catalyst containing supported gold on ytterbium oxide was

identified to be less active (58.1% conversion) but more selective (69.6% of styrene oxide selectivity) than that of alkaline earth metal oxides [46]. Meanwhile, Pan et al. [26] demonstrated that excellent styrene conversion and styrene oxide selectivity of 89.6% and 89.7%, respectively can be obtained using maghemite-supported Ag in ethyl acetate.

1.6.4(a) Zeolites as a catalyst support

Microporous zeolite is another option for supporting active metal centres. Silva et al. reported that manganese(II) salen complexes encapsulated complexes in zeolite NaX and NaY were able to epoxidize styrene [47]. Meanwhile, Co(II)-azamacrocyclic complexes encapsulated zeolite Y can catalyse the conversion of styrene to styrene oxide with 65.2% conversion and 86.5% epoxide selectivity [48]. Nevertheless, metal cations can also be incorporated into zeolite by direct synthesis or ion exchange pathway. For instance, cubic porous zeolite A supported Ag prepared *via* ion exchange in supercritical carbon dioxide was proven active towards styrene epoxidation with up to 83% conversion [49]. Similar zeolite 4A supported Ag catalyst prepared by one-pot hydrothermal synthesis achieved 80.8% conversion and 89.2% epoxide selectivity [50]. A research conducted by Tang and his co-workers [51] to investigate styrene epoxidation activity of cobalt exchanged zeolite NaX revealed that the prepared cobalt zeolite X has moderate activity and selectivity towards epoxide formation. Although the selectivity of this catalyst is comparable when using molecular oxygen and hydrogen peroxide, its catalytic activity is higher with molecular oxygen acting as oxidant.

Introducing more than one type of metal cation can generate a synergistic effect on the epoxidation performance of zeolite supported catalyst. The single and most

successful example is the alkali earth metal promoted Co-exchanged X catalytic system developed by Sebastian, and co-workers [27]. The outcome of their research showed that cobalt cation is mainly responsible for the high conversion (~100%) while alkali and alkaline earth metals can be introduced to enhanced styrene oxide selectivity. It is proven that alkaline earth metals are more effective in enhancing the selectivity of Co-X than alkali metal cations. Comparable selectivity of 83-85% can be achieved by exchanging the framework sodium cation with calcium, strontium or barium. This method has been patented in the United States and Europe [52,53]. The limitation in styrene oxide selectivity is the high operating temperature of 100 °C, which facilitates the decomposition of styrene oxide.

1.6.4(b) Mesoporous silica as catalyst support

Mesoporous silicas are silicate materials containing ordered mesopores, which have pore size between 2-50 nm. Since the first discovery of MCM-41 by the researchers of Mobil Corporation, various types of mesoporous silicas have been successfully prepared, including MCM-48, SBA-15, SBA-16, KIT-6, and TUD-1. These mesoporous compounds were extensively examined for their applications as support, catalyst, and adsorbent. Numerous works have been reported on the catalytic activity of metal supported on mesoporous silica in styrene epoxidation. Pachamuthu et al. [54] directly synthesized foam-like disorder silica (TUD-1) containing copper cation for styrene epoxidation. Their results showed that the mesoporous silica itself is inactive towards the reaction. The inclusion of copper significantly improves styrene conversion. Although the conversion is proportional to the amount of copper cation, a higher amount of copper will adversely reduce the selectivity towards styrene oxide due to the formation of bulk CuO

species. The highest conversion and selectivity achieved under optimum condition were 74.8% and 57.1%, respectively. On the other hand, incorporation of indium oxide on TUD-1 can catalyse the epoxidation of styrene with up to 60% of epoxide selectivity and approximately 25% of conversion when molecular oxygen was used [55].

Recent research by Li and his colleagues [56] using Cu(II)-Co₃O₄ supported on three-dimensional cubic mesoporous KIT-6 reveals that supported Co₃O₄ spinel phase doped with Cu perform better than supported mix phase of CuO and Co₃O₄. The catalyst with a moderate molar ratio of Cu/Co=1/8 reached the highest conversion and styrene oxide selectivity of 53.8% and 82.6%, respectively. Their findings evidenced that instead of textural properties, the chemical environment of active metal sites dominates the catalytic activity of the catalyst. Another research group reported the use of one-pot hydrothermal synthesized Zr-Mn/MCM-41 for styrene epoxidation using TBHP [57]. It was shown that Mn/MCM-41 achieved high styrene oxide selectivity with a little conversion. Adding zirconium eventually increases both the conversion and selectivity of the catalytic reaction. However, the improvement in conversion is more prominent than that on the selectivity. In this system, 41.2% of conversion and 87.35% of styrene oxide selectivity were attained.

Several studies have been done on the use of mesoporous silica encapsulated metal complexes. Styrene epoxidation in the presence of peroxophosphotungstate/SBA-15 (POM/SBA-15) achieved total styrene conversion and 100% styrene oxide selectivity in only two hours of reaction time and at mild condition [28]. Although this catalyst experience negligible leaching of metal active sites, its selectivity drops to 60% after four catalytic reactions. Moreover, the designed system required both H₂O₂ and O₂ as the

oxidant for the reaction, which can incur extra cost on production set up, maintenance and occupational health and safety investment. An experiment carried out by Rahiman et al. [58] demonstrated the catalytic performance of iron(III) porphyrin encapsulated into Al/Ti/V-MCM-41 by ion-exchange method. The results indicated that FeTAPP achieves 46.0% of epoxide yield when attached to V-MCM-41. This result is higher than that of using Ti-MCM-41 (39.2%), Al-MCM-41 (10.3%) and MCM-41 (17.3%) as support.

Zhang and his colleagues studied the encapsulation of chiral ruthenium porphyrin [Ru(II)(D4-Por*)CO] on silica, silica gel, MCM-41 and MCM-48 [59]. Optimum epoxide yield of 86% was obtained with the use of three-dimensional MCM-48 support. The challenges faced when using this MCM-48 supported catalyst include poor reusability, tedious catalyst preparation protocol and the need to replace highly volatile dichloromethane with greener solvent. In addition to network type, the catalytic performance of the supported catalyst was also governed by the pore size, channel type and adsorbent-adsorbate interaction. This is described by Wang and his co-workers who studied styrene epoxidation with H₂O₂ catalysed by alanine–salicylaldehyde Schiff base chromium(III) complexes immobilized on mesoporous silicas [60]. After comparing the result between MCM-41 and SBA-15 supported complexes, their works revealed that methyl-containing alanine–salicylaldehyde chromium(III) MCM-41, which possesses smaller pore diameter and uniform parallel channel, achieved lower conversion but higher epoxide selectivity than the crossed channel, big pore size SBA-15 counterparts. This is because the latter exerts stronger adsorption on styrene and epoxide molecules, which allowed these molecules to approach the active sites more easily. Consequently, higher conversion of styrene and lower epoxide selectivity was observed in SBA-15 supported

samples. The highest conversion and selectivity recorded were 80.2% and 77.0%. The performance of catalyst gradually decreases for the first four cycles of reactions and experiences dramatic decline since then. This is rationalized as the result of active site blockage by residual adsorbed molecules.

The influence of metals on the catalytic performance of mesoporous silica supported metal complexes has been investigated by different research groups. Sun et al. [61] demonstrated that copper(II) Schiff anchored onto amino-functioned KIT-6 achieved the best catalytic performance of 98.6% of conversion and 97.8% of styrene oxide selectivity when compared to Fe^{2+} , Co^{2+} , Ni^{2+} and VO^{2+} counterparts. The selectivity is 11.8% higher than the one grafted on MCM-41 [62]. It is expressed that the KIT-6 support is responsible for the inhibition of dimerization, which enhanced the catalytic performance of Cu-salen supported on it. This is consistent with the previous finding of Tang et al. [63] who showed that Cu supported on mesoporous silica nanoparticles (MSN) achieved higher conversion and selectivity than the Co-MSN and Mn-MSN.

1.6.4(c) Other supports

Apart from the above category of support, there is a vast variety of materials being tested as a catalyst support in styrene epoxidation. Barium titanate nanotubes (BaTNT) has been used to support gold particles for styrene epoxidation with peroxides. Nepak and Srinivas [64] reported that 1 wt% Au supported on BaTNT can selectively convert 60.5% of styrene with an epoxide selectivity of 80.1% by using TBHP.

Layered double hydroxides (LDH) comprising of a layer of metal cations sandwiched by two layers of a hydroxide ion and intercalating anions is another type of

support that has been used to support metal active sites. It was reported by Wang et al. [31] that Ag nanoparticles supported on MgAl-LDH with Ag loading of 2.76 wt% can oxidize 80.8% of styrene with up to 91.1% epoxide selectivity at optimized conditions. Meanwhile, gold nanoparticles supported on MgAl-LDH has demonstrated to be an efficient catalyst in the epoxidation of styrene by achieving 51.5% of styrene oxide yield and turnover frequency of 479.1 h at an Au loading of as low as 0.22 wt% [65]. Another study using Y^{3+} modified MgAl-hydrotalcite as a catalyst has shown that the catalytic activity of the metal-supported LDH depends on its basicity [10].

Minerals can also be used to support metal active centres for styrene epoxidation catalysis. Liu et al. [30] have investigated the catalytic activity of Au_{25} cluster supported on hydroxyapatite in the epoxidation of styrene. The catalyst efficiently converts 100% of styrene at 92% selectivity when using toluene as solvent and TBHP as oxidant at optimum condition. Nevertheless, mineral clay has also been used to support metal complex in catalysing styrene epoxidation. Cationic manganese (III)-salen complex was supported on K10-montmorillonite by Kuźniarska-Biernacka and her co-workers [66] and tested for its catalytic activity in epoxidizing three different alkenes. They managed to obtain 99% of styrene conversion and 93% of epoxide selectivity under a m-chloroperoxybenzoic acid (m-CPBA) and N-methylmorpholine (NMO) oxidant system. Another group obtained 60% of styrene conversion and 58% of epoxide selectivity when heteropolymolybdate nanoparticles supported between silicate layers of bentonite was used [67]. On the other hand, Wang et al. observed 65.5% of styrene conversion and 89.7% of styrene oxide selectivity when Pd-palygorskite was used as catalyst in the styrene epoxidation [68].

These examples demonstrated that minerals, especially clay materials, are potential support to the preparation of metal-based catalysts for styrene epoxidation.

Carbon-based support is another option that has been extensively investigated. An experiment conducted by Lebedeva and her colleagues showed that fullerene-derivatized Cu(II) salen complex anchored inside hollow graphitized carbon nanofibers (GNF) can completely oxidize styrene and yield 42% of epoxide in the presence tertbutyl hydroperoxide [69]. Additionally, transition metal-based complexes, for instance, oxovanadium(IV), iron(III), copper(II), and cobalt(II) salen complexes immobilized on native or functionalized graphene oxide have been used for aerobic epoxidation of styrene [70,71]. Amongst these complexes, copper(II) salen complex supported on graphene oxide achieved the optimal yield with 73.5% of styrene conversion and 54.1% of styrene oxide selectivity [71]. Other examples of styrene epoxidation catalyst with carbon-based support include MgO-carbon composite [32], Ag/carbon nanofibers [72], Mn(III) salen complex supported on activated carbon [73], CoFe Prussian blue analogue/carbon nanotube [74], Co/carbon nanotube [75] and Au/carbon nanotube [76]. The catalytic performance of these catalysts is between 21.4%-84.0% for styrene conversion and between 45.2%-82.0% for epoxide selectivity. Ag/Carbon nanotubes have the lowest activity and selectivity while MgO/carbon composite performs the best with 84.0% of conversion and 82.0% of epoxide selectivity. This suggested that alkaline earth metal can be a more active and more selective metal active site than transitional metal.

1.7 Reaction mechanism

Understanding the reaction pathway is important for the formulation of an efficient catalyst. The reaction pathway depends on the chemical nature of the metal active sites and the oxidant system. The reaction mechanism involving the use of hydrogen peroxide is of particular interest since it is more reactive than molecular oxygen, safer to handle and produces only water as the sole by-product.

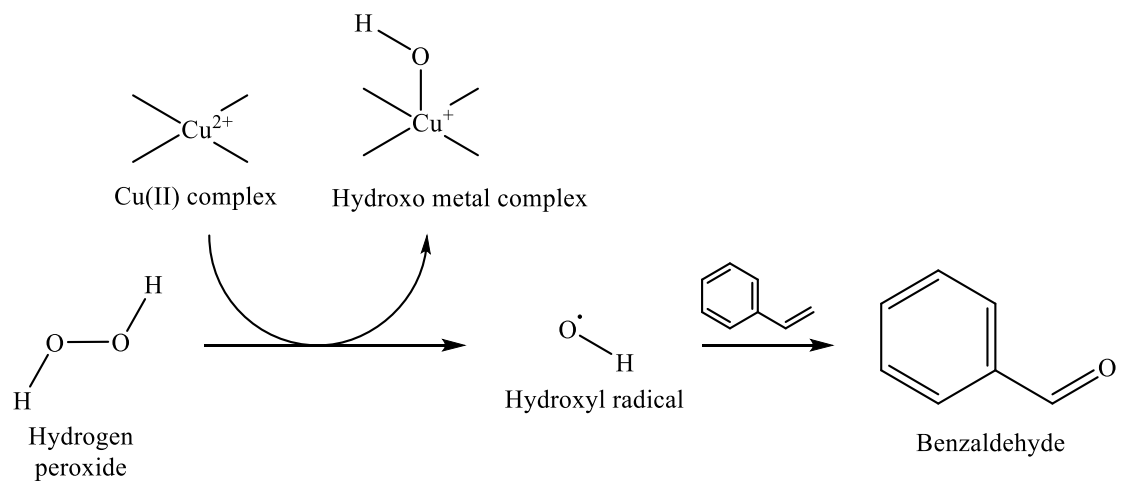
The type of metal in a catalyst has a large influence on the behaviour of hydrogen peroxides [77]. One-electron redox system will lead to the homolytic cleavage of hydrogen peroxide which produces hydroxyl radical. In the presence of iron, the process is known as the Fenton reaction. This was demonstrated by the work of Duarte et al. [78] which used a C-scorpionate Cu(II) complex to catalyse the oxidation of styrene to benzaldehyde (Figure 1.3(a)).

Earlier review of the epoxidation reactions catalysed by transition metals (M) has described the formation of M-OOH as the result of the heterolysis of hydrogen peroxide. Complexes of transition elements in a high oxidation state, for instance, titanium(IV), vanadium(V), molybdenum(VI), and tungsten(VI), can facilitate the heterolysis of hydrogen peroxide by forming complexes analogous to the inorganic peracids (Figure 1.3(b)) [21]. These metals act as a Lewis acid and are labile to ligand substitution. The hydrogen peroxide attracted to the metal centre can be coordinated through monodentate or bidentate mode.

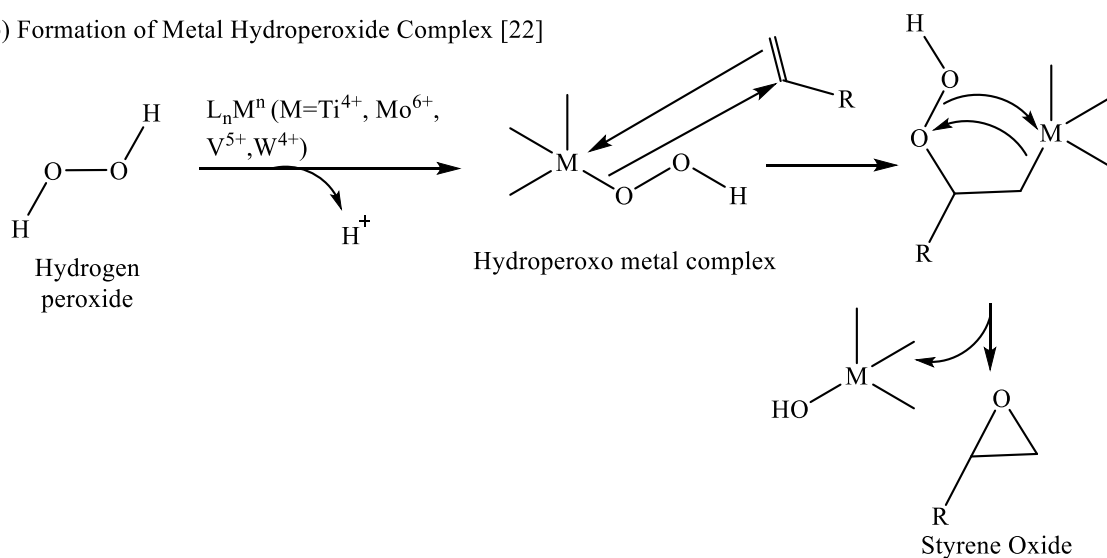
A separate example of hydrogen peroxide heterolysis was demonstrated by Nakagawa and Mizuno [79] using a divanadium-substituted polyoxotungstate [γ -

$\text{H}_2\text{SiV}_2\text{W}_{10}\text{O}_{40}]^{4-}$ catalyst. The bimetallic catalyst dissociates hydrogen peroxide to form hydroperoxide anion and proton. The latter was combined with the hydroxide ligand of catalyst and removed as water molecules. A similar heterolytic epoxidation mechanism was observed when using main group metal oxide. It was proposed that the surface hydroxyl group of calcium will abstract a proton from hydrogen peroxide to form hydroperoxide anion and water (Figure 1.3(c)) [25].

a) One-Electron Transfer [79]



b) Formation of Metal Hydroperoxide Complex [22]



c) Formation of Metal Hydroperoxide [26]

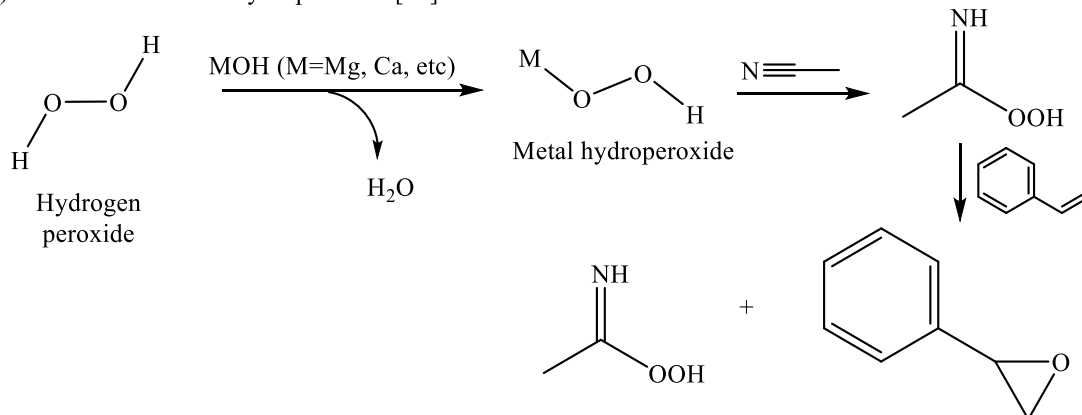


Figure 1.3 Reaction mechanism of hydrogen peroxide activation through (a) one-electron transfer [79], (b) formation of metal hydroperoxide complex [22], and (c) formation of metal hydroperoxide [26].

1.8 Mesoporous silica support

Mesoporous silicas are silicate materials that contain mesopores (2-50 nm). Numerous types of mesoporous silicas have been discovered since the discovery of MCM-41, which includes MCM-48, SBA-15, SBA-16, KIT-6, and HMS-5. They are interesting because of their tuneable pore diameter, large surface area, and uniform pore structure [80,81]. These attributes overcome the shortcoming of zeolites which possess mass transfer limitation [82]. The latter contains only small pore volume and pore size that make it ineffective in catalysing reactions involving large molecules.

Typically, mesoporous silica, for example, MCM-41, SBA-15, and SBA-16 can be synthesized through a liquid crystal templating method. The formation of MCM-41, for instance, as illustrated in Figure 1.4 [83]. A structure-directing agent (SDA), which is known as cetyltrimethylammonium bromide (CTAB), is added to produce micelles that act as the template in the synthesis process [84,85]. As an amphiphilic molecule, the polar head groups of the SDA will face towards the external aqueous environment while its hydrophobic hydrocarbon tail will face inwards. Depending on the type and charges of head groups, different silica sources can be introduced. The dissolved silicate species undergo self-assembly by being electrostatically attracted to the surface of pre-formed micelles. These silicates are then condensed to form a well-defined polysilicate framework when subjected to hydrothermal conditions. At the end of synthesis, the excess template can be washed away with solvent (water, acetone or ethanol). The filtered mesoporous silica will then be subjected to calcination to remove existing liquid crystal templates and recover the mesopores.

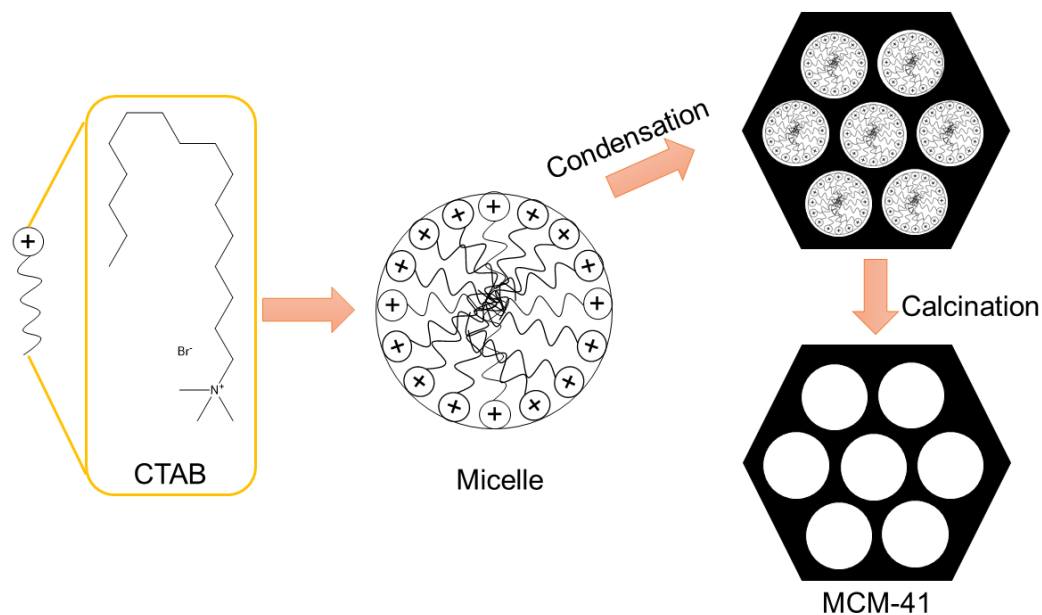


Figure 1.4 Schematic presentation of MCM-41 synthesis, an example of liquid crystal templating synthesis of mesoporous silica [83].

Several factors have been identified to govern the formation of mesoporous silica. It was found that the amount and chemical properties of SDA are the determinants of the shape, pore size distribution, morphology and order of mesoporous silica [86]. In a study, Renuka and her colleagues evaluated the influence of CTAB concentration on mesoporous silica synthesis [87]. Their study demonstrated that SBA-16 was formed instead of MCM-41 by simply diluting the CTAB solution while maintaining other experimental parameters. Meanwhile, an experiment conducted by Lin et al. [88] showed the carbon chain length of SDA could influence the structure and porosity of prepared mesoporous silica. The pore size and wall thickness of resulting MCM-41 were found to increase with increasing carbon chain length of SDA. Besides that, it was also proven that increasing surfactant content can rise the unit cell parameter of MCM-41. The study concluded that the optimum range of surfactant/SiO₂ ratio falls within 0.09-0.15.

Additionally, synthesis temperature can also affect the lattice parameter of mesoporous silica. A study by Corma and his colleagues[89] revealed that increasing synthesis temperature from 135 °C to 175 °C improved the lattice parameter and shortened the crystallization time of MCM-41. The same study demonstrated that stirring could promote the formation of the ordered mesoporous structure while reducing crystallization time.

1.8.1 Metal Incorporated Silica

Introducing metal into mesoporous silica can be used to modify their physicochemical and catalytic properties. Approaches such as wet impregnation, ion exchange, chemical vapour deposition (CVD), and direct one-pot synthesis have been studied [90–92]. Among these methods, direct one-pot synthesis has been shown to be a promising modification pathway owing to its simplicity. However, the influence of metal on mesoporous silica formation needs to be determined and understood in order to produce a catalyst with optimized efficiency.

Many works have been done to study the effect of direct metal incorporation on the morphology of the resulting catalyst. An investigation reported by Mokhonoana on the direct synthesis of Fe-MCM-41 demonstrated that the mesoporous long-range order of MCM-41 diminished with an increasing amount of Fe added to the reaction mixture containing water glass, CTAB, and H₂O [93]. Although a long-range pore channel order can be preserved when Fe metal was precipitated with hydroxide before being added to the synthesis solution, undesired structural destruction and pore blockage occurred when metal loading was beyond 20 wt%.